Comparative study of effectiveness between MPPT regulations with optimal TSR and with neuro-fuzzy in the face of the torque impact of a Vertical Axis tidal turbines column with a PMSG

Télesphore RANDRIAMAITSO[1*], RHEVIHAJA[2], F. Philibert ANDRINIRINIAIMALAZA[1], and Théodore TOTOZAFINY[3]

[1]*University of Mahajanga, Higher Institute of Sciences and Technologies, Ex-LOLO Building Mahajanga-be, Madagascar*
[2]*University of Mahajanga, EDGVM Doctoral School, Madagascar*
[3]*University of Mahajanga, Faculty of Sciences, Technologies and Environment, Madagascar*

ABSTRACT

The objective of this article is to compare the effectiveness between the optimal TSR MPPT regulation strategy and the neuro-fuzzy MPPT one to control the column of turbines of a vertical axis tidal turbine facing the impact of its oscillated torque on the electromechanical quantities output of the PMSG such as rotational speed, currents and voltages. In this study, the turbine torque is determined by the DMST method. And, the Park model of the PMSG is used. In addition, the methods of regulating the turbine by the optimal TSR MPPT and by the neuro-fuzzy MPPT are studied. Each control strategy includes PI correctors and a PWM rectifier in the electrical chain. Three turbines mounted in a column with the same radius of 455mm and height of 824mm were considered. The simulation was carried out with operation at maximum average efficiency of the column of three turbines and a flow of 1.5 m/s. Without a control system, the rotational speed of the PMSG with the three non-offset turbines, when feeding a resistive and inductive load, has the amplitude more wavy compared to if they are offset. The output quantities of PMSG are improved by both regulation strategies. The MPPT neuro-fuzzy regulation mode is more effective than the MPPT one at optimal TSR. Due to the fact that the turbine produces the oscillating speed and that, unlike the MPPT strategy at optimal TSR, the MPPT neuro regulation mode -Fuzzy provides instant reference speed. A comparative study with other regulation strategies using instantaneous reference rotation speeds can be undertaken.

Keyword: -*Tidal turbines column, vertical axis, PMSG, Optimal TSR, neuro-fuzzy, electromechanical output.*

---

1. INTRODUCTION

Currently, the energy we use daily comes mainly from usual sources such as fossil fuels (oil, gas, coal) [1], [2]. Their major disadvantage lies in the very rapid exhaustion and the emission of gases which enormously pollute the atmosphere. Faced with the constraints posed by fossil fuels, the best possible solution would be to use renewable energies which have the advantage of being abundant and inexhaustible in the millennia to come. It is in this situation that tidal energy presents itself today as one of the most interesting sources of renewable energy, thanks to its enormous potential [3].

Tidal turbines are turbines that recover kinetic energy from river or sea currents. They are somehow equivalent to wind turbines. To produce energy, tidal turbines will need a current speed greater than 1m/s on average [4].

The Permanent Magnet Synchronous Machine (PMSM) is widely used in tidal turbine applications, in particular, because of its good conversion efficiency (close to 99% compared to the asynchronous machine) [4]. The PMSM allows operation at both low speed (direct drive system) and high speed (indirect drive system), so it can be coupled or not with a speed multiplier [5]. Two main categories of tidal turbines exist: those with a horizontal axis of rotation and those with a vertical axis of rotation. This study considers a tidal turbine with a vertical axis of rotation equipped with a direct-drive permanent magnet synchronous generator (PMSG). The PMSG transforms mechanical energy into electrical energy. Studies show that the vertical turbine provides pulsating torque [2] [6] [7] [8] [9] [10].

So, our objective is to compare, by simulation, the efficiency between the optimal TSR (tip speed ratio) MPPT (Maximum Power Point Tracking) control [11] and the neuro-fuzzy MPPT [12] [13], under the impact of the vertical axis turbines column's torque oscillation on the output quantities of a PMSG. The simulation requires the modeling of the tidal turbines column system without or including the MPPT control strategy with PI corrector [14] [15], the vector control of the PMSG associated with PI corrector and the MLI rectifier based on bipolar transistor (IGBT) [16] [17] [18]. Then, the torque of the turbines column is determined by the Double Multiple Stream Tube (DMST) method [2] [4] [6] [19] [20] [21] [22]. Finally, the PMSG PARK model [23] [24] is used.

In the section 2, material and methods are presented. In which, firstly, the under study system is defined and is described as well as its architecture. Secondly, the used algorithm controllers are explained for an optimal TSR MPPT control, and for a neuro-fuzzy control strategies. Simulation results are delighted in section 3 followed by discussions for the details of contribution in section 4. Finally, in the last section, conclusions are given.

2. MATERIAL AND METHODS

2.1 Presentation of the studied system

The tidal turbine considered comprises three-phase PMSG and the column of three vertical axis turbines, each turbine of which is three straight blades of height H, radius R, profile NACA0018 [25] and chord length C according

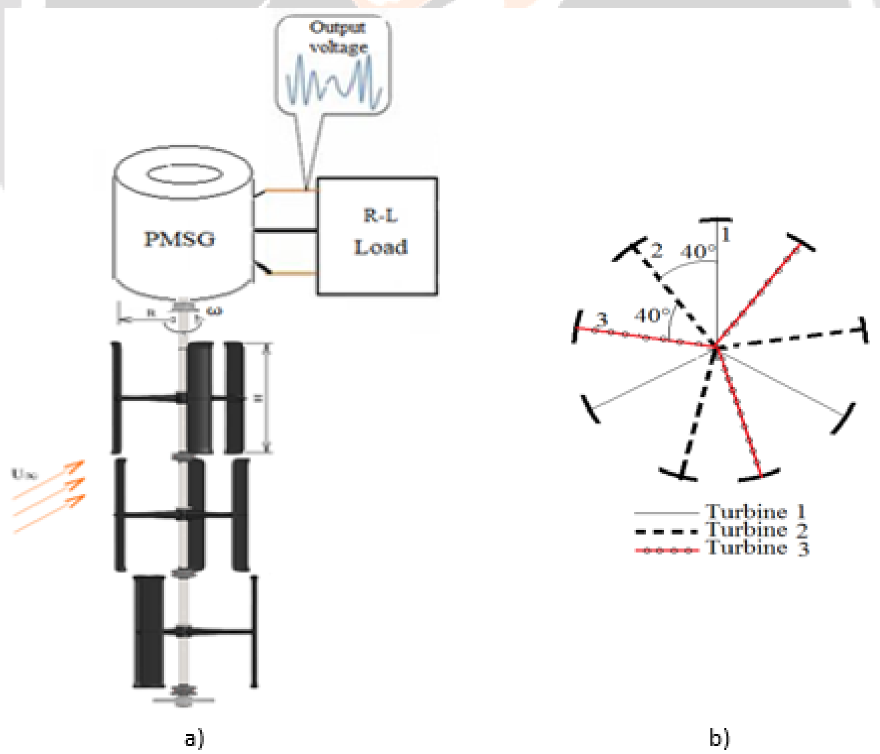

Fig -1: Presentation of the tidal turbines column b) View from the top of the column of three turbines when they are offset

to Fig-1. The column of turbines is placed in a flow of speed $\vec{U}_\infty$assumed to be constant and uniform and rotates with a rotation speed ω fixed by the electric generator. The latter provides currents and voltages characterized by a frequency and amplitudes. It powers an RL load.Fig -1-b shows the three turbines when they are offset by 40° [2].

2.2Turbine modeling

2.2.1 Power coefficient and tip speed ratio (TSR)

The mechanical power $P_m$that can be produced by a tidal turbine represents a fraction $C_P$of fluid'shydrodynamic power, in formula (1).

$$P_m = \frac{1}{2} C_P \rho A U_\infty^3 \quad (1)$$

WhereC_P is the power coefficient characterizing the hydrodynamic performance of a tidal turbine, ρ the density of water (kg/m3), A the surface swept by the blades (m2), and $U_\infty$the tidal speed (m/s). The coefficient of power $C_P$does not exceed the limit of 59% which constitutes the Betz limit [18].

Figure 2 presents the evolution of the power coefficient according to the tip speed ratio λ which is expressed by equation (2).

$$\lambda = \frac{\omega R}{U_\infty} \quad (2)$$

The optimum value of the tip speed ratio (λ_{opt}) corresponding to the maximum power coefficient is a characteristic of the turbine.

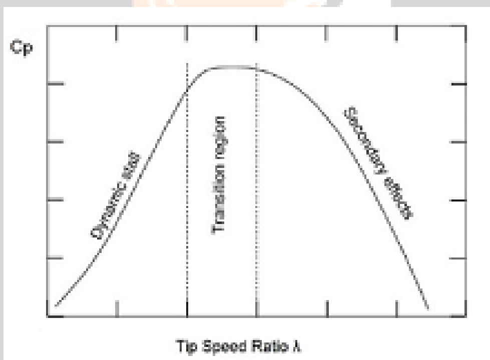

Fig -2: Evolution of the power coefficient as a function of the advance parameter [7]

To control a turbine, the reference speed for optimal MPPT TSR control method is given by formula (3) [15].

$$\omega_{réf} = \frac{\lambda_{opt} U_\infty}{R} \quad (3)$$

2.2.1 Forces and speeds

The blade placed in a flow is subjected to two forces (Figure 3): the drag force parallel to the direction of the flow, denoted D, and the lift force perpendicular to the flow and denoted L.

On the other hand, the force $\vec{F}_N$is a decisive force for the mechanical resistance of the blades because it is very variable and generates an alternating loading on the blade. The rotor surface can be divided into four zones: two driving zones and two braking zones. The surface of the rotor can be broken down into four zones: two motor zones and two braking. These two driving zones are located in part of the upstream half-disc and part of the downstream half-disc of the turbine according to Figure 4.

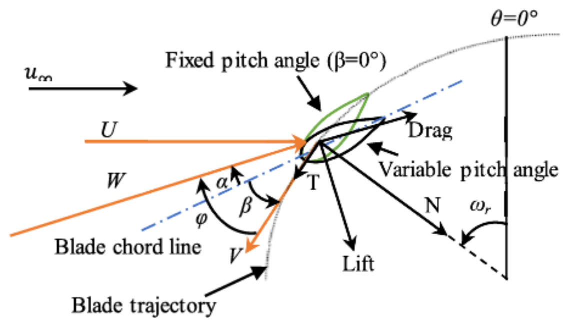

Fig -3: Forces and velocities acting on the blade of a turbine [23]

Where angles α, β, and θ are respectively angle of attack or angle of incidence, a pitch angle, and the azimuth angle. The available torque on a tidal turbine is given by the force $\vec{F}_T$, tangential to the circle of rotation.

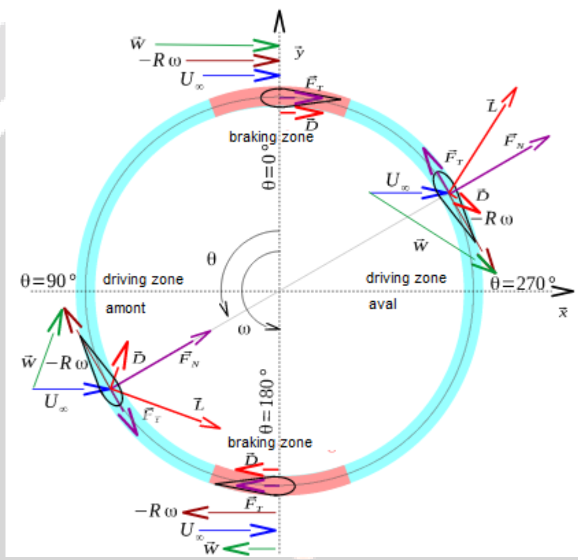

Figure 1: Analysis of driving and braking zones in a vertical axis turbine [18]

2.2.3 Determining the torque, power and efficiency of a vertical axis tidal turbine using the DMST model

Figure 5 represents the tidal turbine modeled by two upstream and downstream actuator discs.

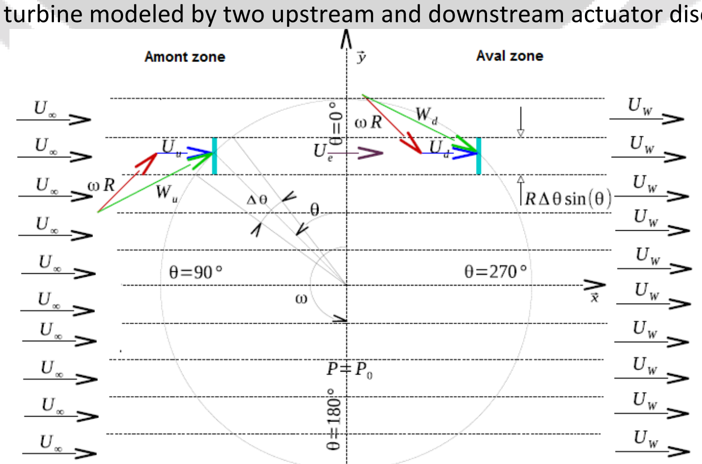

Figure 2: Model with multiple current tubes and two actuators (seen from above) [18]

There is an equilibrium position located between the upstream zone and the downstream zone whose speed of passage in this zone is called equilibrium speedU_e. When the fluid passes through this zone, the pressure is equal to that of the undistributed flow upstream of the turbine.

The induction factors $a_u$anda_d respectively of the upstream and downstream half-disk are defined by relations (4) and (5).

$$a_u = \frac{U_\infty - U_u}{U_\infty} \tag{4}$$

$$a_d = \frac{U_e - U_d}{U_\infty} \tag{5}$$

The DMST model using the laws of fluid mechanics with the actuator disk theory allows to establish non-linear equations relating the induction factors, the hydrodynamic parameters and the geometric parameters of the turbine.

$$a_{u,\,d} = \begin{cases} \tilde{F}_{x\,u,\,d} + \quad a_{u,\,d}^2 & 0.0 \leq a_{u,\,d} \leq {}^1\!/_3 \\ \tilde{F}_{x\,u,\,d} + \frac{1}{4}(5 - 3a_{u,\,d})a_{u,\,d} & {}^1\!/_3 < a_{u,\,d} \leq 1.0 \end{cases} \tag{6}$$

$$\tilde{F}_{xu} = \frac{B\ C}{8\pi R\ |sin(\theta)|}\left(\frac{W_u}{U_\infty}\right)^2 (C_n sin\theta - C_t cos\theta) \tag{7}$$

$$\tilde{F}_{x\,d} = \frac{B\ C}{8\pi\rho R\ |sin(\theta)|}\left(\frac{W_d}{U_\infty(1 - 2a_u)}\right)^2 (C_n sin\theta - C_t cos\theta) \tag{8}$$

The resolution of the equations obtained is done by the iterative numerical method and results in obtaining adimensional coefficient $C_t$of the tangential force T and the relative speed $W_{u,d}$. Therefore, we can calculate the torque for a blade with respect to the axis of rotation according to the following formula:

$$T_i(\theta) = \frac{1}{2}\rho W_{u,d}^2 (HC) C_t R \tag{9}$$

For a tidal turbine with B blades, the instantaneous global torque provided by the blades will be determined by equation (10) [4] and [18].

$$T(\theta) = \sum_{i=1}^{B} T_i(\theta_i)\,, avec\ \theta_{i+1} = \theta_i + \frac{360}{B} \tag{10}$$

The average torques for the upstream and downstream half-discs of the turbine are respectively evaluated by the following equation (11) and equation (12) [19]:

$$T_{avg,u} = B \sum_{i=1}^{N_\theta} \frac{\left(\frac{1}{2}\rho W_u^2 (HC) C_t R\right)}{N_\theta} \tag{11}$$

$$T_{avg,d} = B \sum_{i=1}^{N_\theta} \frac{\left(\frac{1}{2}\rho W_d^2 (HC) C_t R\right)}{N_\theta} \tag{12}$$

The average total torque of the tidal turbine over one revolution can be expressed by equation (13).

$$T_{avg} = \frac{1}{2}(T_{avg,u} + T_{avg,d}) \tag{13}$$

The torque and power coefficients are calculated respectively by the following equations (14) and (15) [19] [23]:

$$C_{T_{avg}} = \frac{T_{avg}}{\frac{1}{2}\rho U_\infty^2 (2RH)R} \quad (14)$$

$$C_P = \lambda C_{T_{avg}} \quad (15)$$

2.2.4 Determination of the torque and power of a column of vertical axis tidal turbines using the DMST model

For a column made up of three identical turbines, the torque supplied is expressed by [4]:

$$T_{tour}(\theta) = T_{turbine1}(\theta) + T_{turbine2}(\theta) + T_{turbine3}(\theta) \quad (16)$$

Furthermore, for a column made up of three turbines, we will have a total power [4]:

$$P_{tour}(\theta) = P_{turbine1}(\theta) + P_{turbine2}(\theta) + P_{turbine3}(\theta) \quad (17)$$

2.3 PMSG dynamic model in the dq axis

2.3.1 Modeling of the synchronous machine in the two-phase reference frame (dq)

The considered permanent magnet synchronous machine is a radial type magnetization machine with surface mounted magnets.

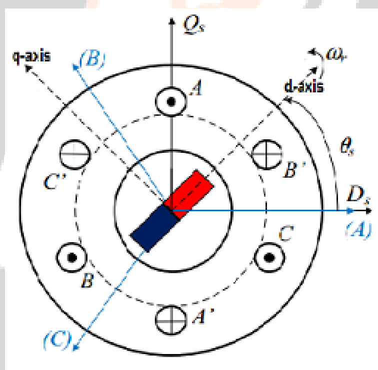

Figure 3: PMSG cross section, Reference frame (a, b, c) and Reference frame (d, q) [12]

Using thegenerating convention, the equations for the machine voltage in the Park frame are as follows:

$$\begin{cases} V_d = -R_s i_d - L_d \frac{di_d}{dt} + p\omega L_q i_q \\ V_q = -R_s i_q - L_q \frac{di_q}{dt} - p\omega L_d i_d + p\omega \psi_f \end{cases} \quad (18)$$

The expression of the electromagnetic torque for the cylindrical rotor will be expressed as follows:

$$\boldsymbol{T_{em} = \frac{3}{2} p\psi_f I_{qs}} \quad (19)$$

The differential equation which characterizes the mechanical behavior of the turbine and generator assembly is given by:

$$T_{tur} - T_{em} = J_{tot}\frac{d\Omega_{tur}}{dt} + f_v \Omega_{tur} \quad (20)$$

Which, $J_{tot}$is the total inertia of the turbine and the generator [kg.m^2]; T_{tur}presents the torque of the turbine [Nm],T_{em} is the electromagnetic torque of the generator [Nm]; $f_v$represents the coefficient of viscous friction [kg/s] and Ω_{tur} is the speed of rotation of the turbine or generator [tr/s].

2.3.2Global model of the PMSG under RL load

The overall model of the *PMSG* under load with Z line = 0 is presented in Figure 7.

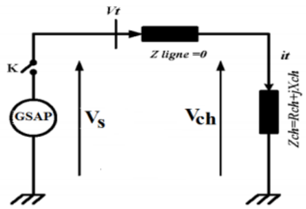

Figure 4: Permanent magnet synchronous generator connected to a load

The R-L load model in the Park frame is [26]:

$$\begin{cases} V_d = R_{ch}\mathrm{i_d} + \mathrm{L_{ch}}\dfrac{d\mathrm{i_d}}{dt} - p\omega\mathrm{L_{ch}}\mathrm{i_q} \\ V_q = R_{ch}\mathrm{i_q} + \mathrm{L_{ch}}\dfrac{d\mathrm{i_q}}{dt} + p\omega\mathrm{L_{ch}}\mathrm{i_d} \end{cases} \quad (21)$$

2.4 Mitigation by controlling the tidal turbine of the Turbine torque impact

2.4.1 Optimal TSR MPPT Control System

Insertion of a control system in the tidal turbine, according to figure 8, makes it possible to improve the output voltage of the generator.The control system is composed of the optimal TSR MPPT control to extract maximum power from the water flow, the PWM command for the rectifier, and the PI correctors for the PMSG regulations.

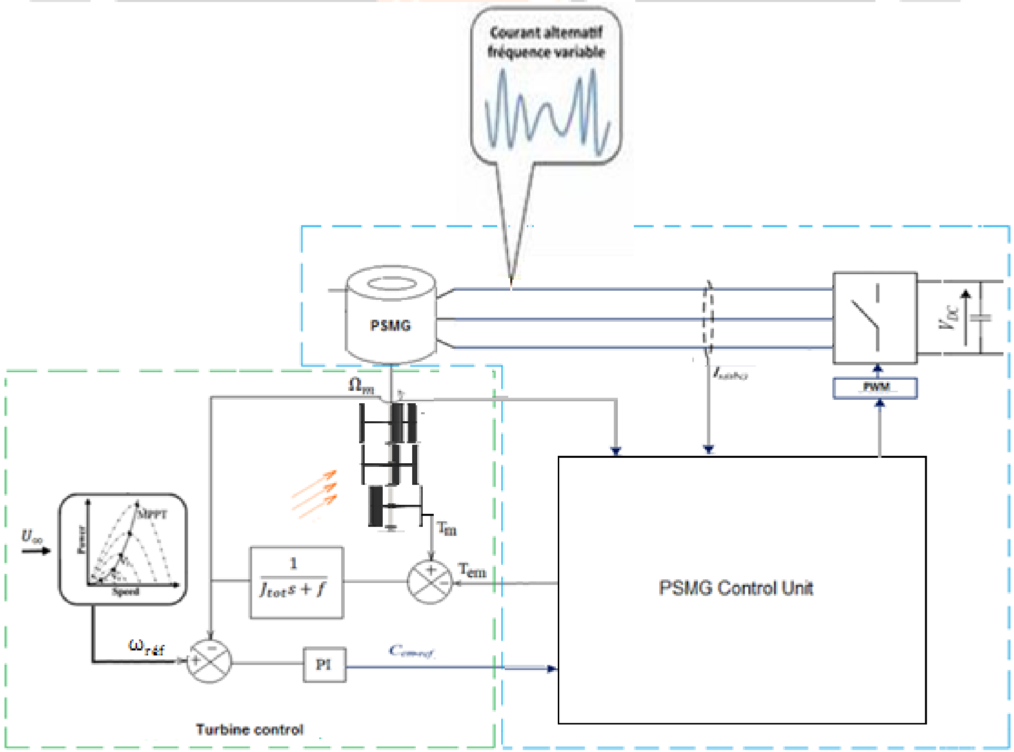

Figure 5: Control of the tidal turbine

2.4.2 Neuro- fuzzy MPPT control system

Figure 9 shows the control of the turbines column by Neuro- fuzzy MPPT. By adopting fuzzy set rules[12][13], the fuzzy MPPT device processes the variation in the extracted power $\Delta P_t$and rotation speed $\Delta\omega_t$at the level of the turbines column which results in a change $\Delta\omega_{réf}$ in the mechanical speed setpoint ω_{tref} of the tidal turbines column.

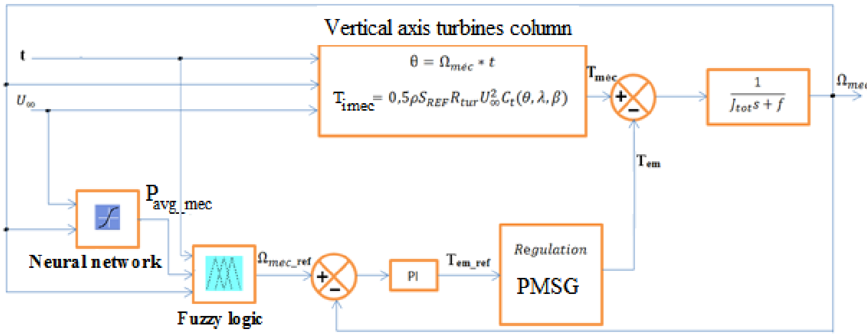

Figure 6: Turbines column control strategy by MPPT Neuro-fuzzy

This is interesting because, even at the constant flow speed, the vertical axis turbine provides an oscillating torque consequently the power varies according to the positions of the blades.The turbines column control system is composed of the neural network to model the power of the turbine column as a function of flow speed and its rotation, and the fuzzy logic MPPT.

3. RESULTS

3.1 Torque and power evolutions

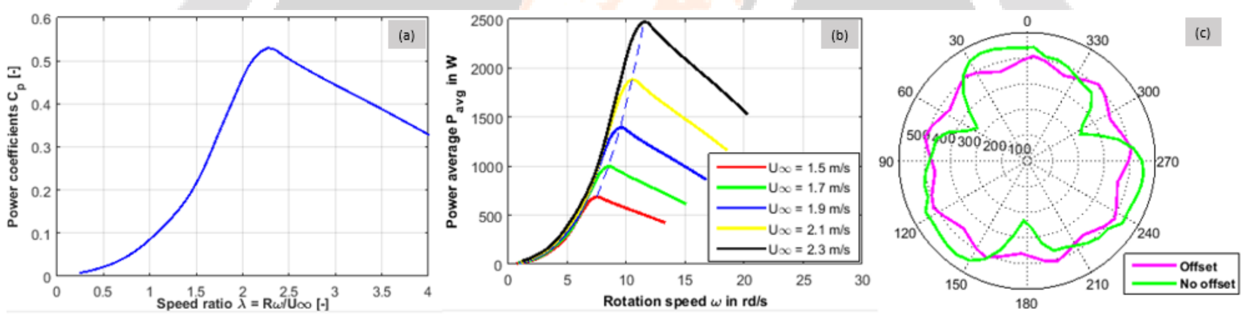

Figure 7: Evolution of (a) the power coefficient as a function of the advance parameter or TSR, (b) Power extracted as a function of flow and rotation speeds, and (c) Torque rosette of the column of three turbines

3.1 Rotation speeds from all configuration

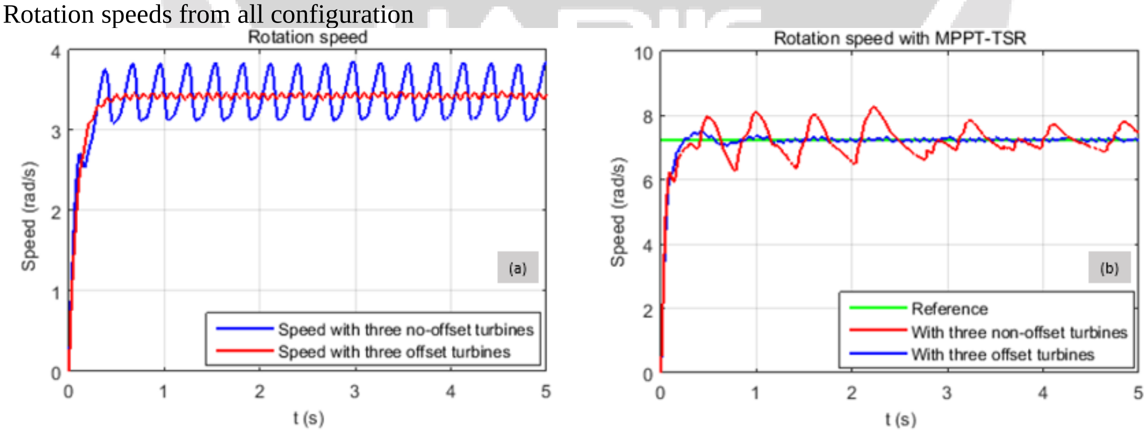

Figure 8: Rotation speeds, (a) in the absence of a control system, (b) withoptimal MPPT-TSR regulation

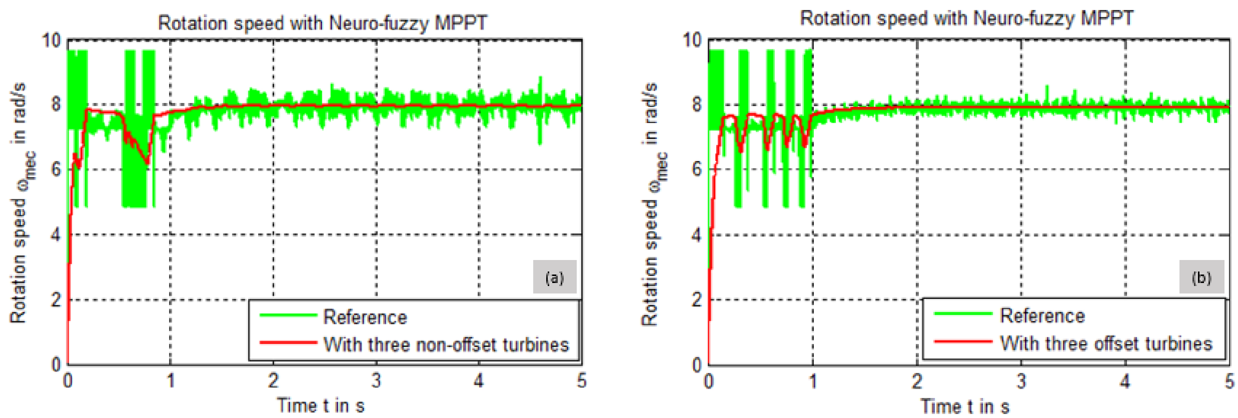

Figure 12 - Rotational speeds With Neuro-fuzzy MPPT regulation of, (a) column of three non-offset turbines, and (b) column of three offset turbines

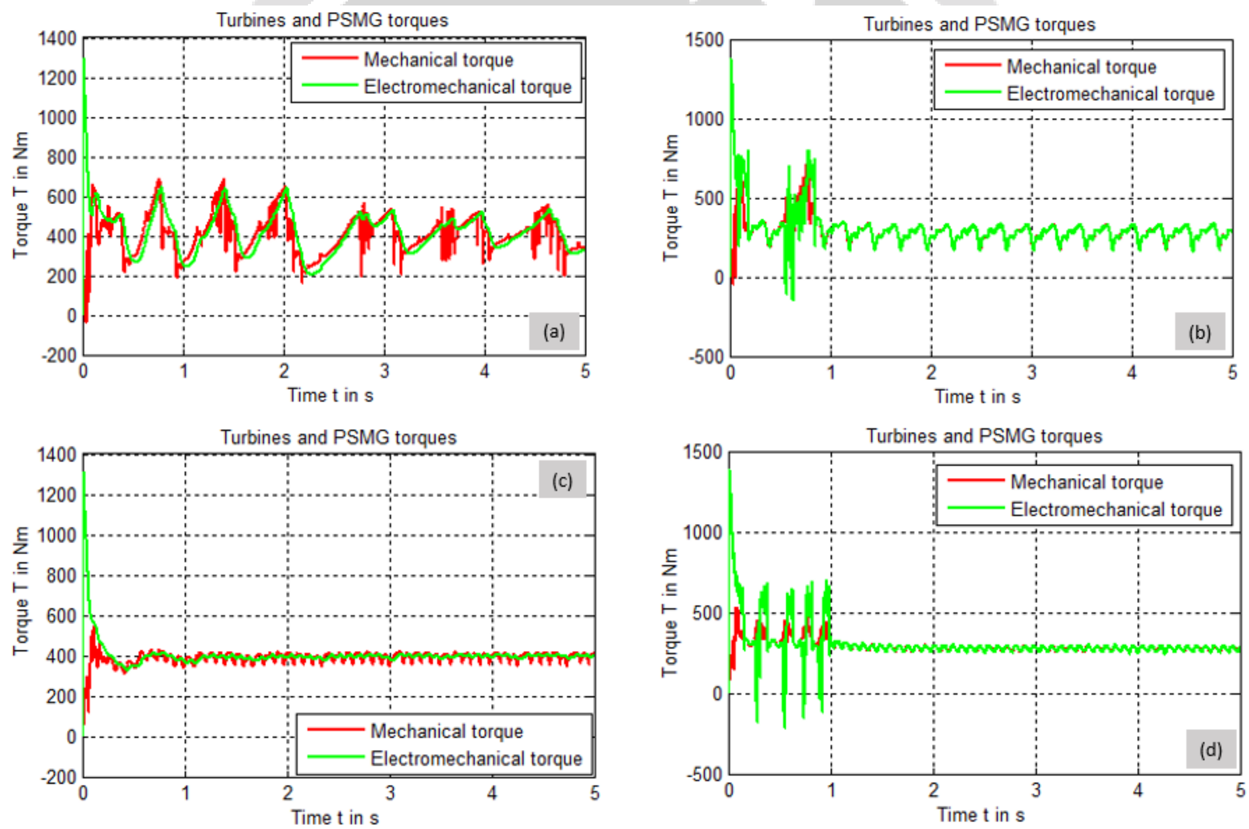

Figure 13–Mechanical and electromechanical torques, respectively, (a) with optimal TSR MPPT regulation and (b) With MPPT Neuro-fuzzy regulation for column of three non-offset turbines, (c) With optimal TSR MPPT regulation and (d) With Neuro-fuzzy MPPT regulation for column of three offset turbines.

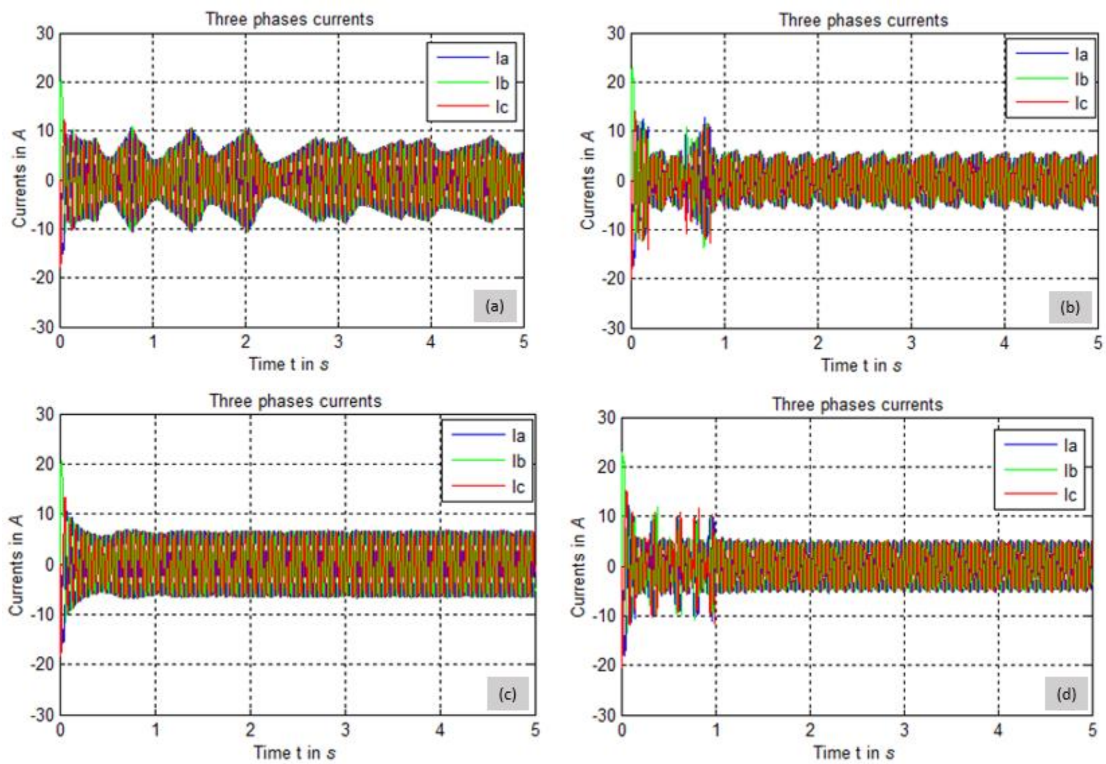

Figure 14–Three phases currents, respectively, (a) with optimal TSR MPPT regulation and (b) With MPPT Neuro-fuzzy regulation for column of three non-offset turbines, (c) With optimal TSR MPPT regulation and (d) With Neuro-fuzzy MPPT regulation for column of three offset turbines.

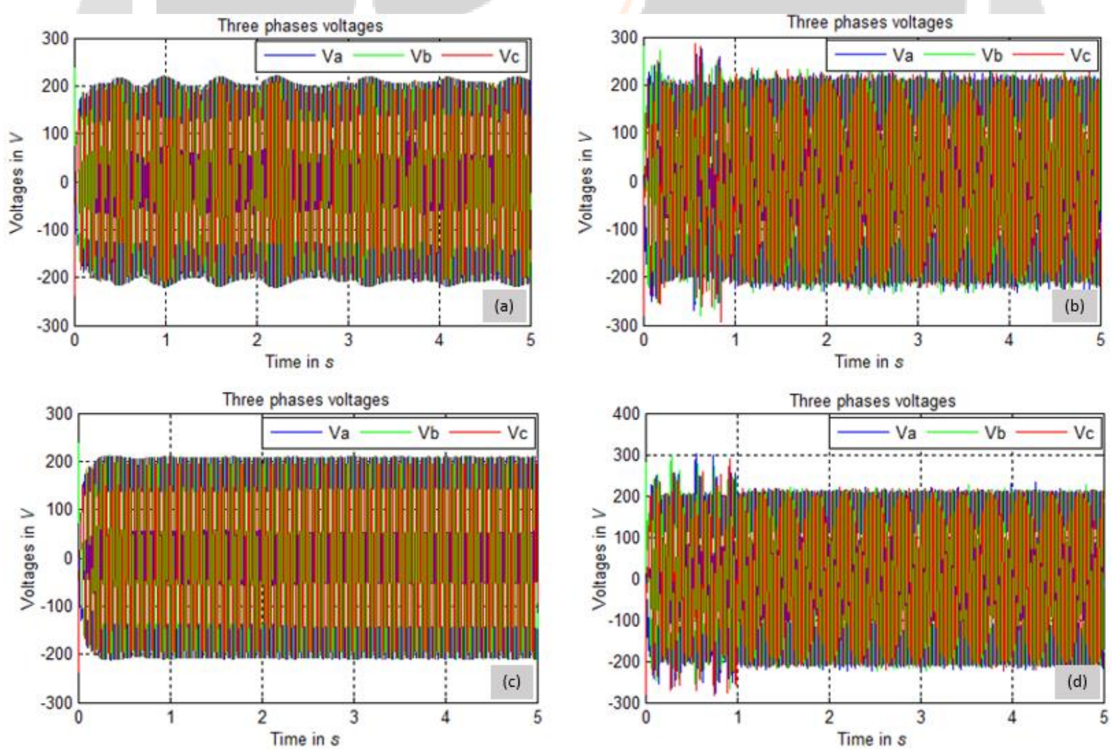

Figure 15–Three phases voltages, respectively, (a) with optimal TSR MPPT regulation and (b) With MPPT Neuro-fuzzy regulation for column of three non-offset turbines, (c) With optimal TSR MPPT regulation and (d) With Neuro-fuzzy MPPT regulation for column of three offset turbines.

4. DISCUSSIONS

The numerical simulation of vertical axis three turbines column based on the DMST method and with the flow $U_{\infty} de\ 1{,}5\ m/s$ was carried out. Figure 10-a shows an evolution of power coefficient CP from 0 to 55.07% being lower than the Betz limit (59.25%). The top of this curve corresponds to the maximum power coefficient (or maximum efficiency) $C_{pmax} of\ 0{,}55$ and the optimal TSR of 2,2 . It constitutes the optimal operating point of the turbine. This result confirms the work carried out by Bossard [27] which shows that the optimal specific speed of tidal turbines is of the order of 2. We note that this power coefficient curve (figure 10-a) has the same appearance predicted in the section 2.2.1 (Figure 2). According to Figure 10– b, we see the different levels of average power as a function of rotation speed which increase following the increase in U_{∞}. This characteristic is exploited in the MPPT (Maximum Power Point Tracking) control strategy of the tidal turbines column, making it possible to extract the maximum power for a flow speed.

At the flow of $U_{\infty} = 1{,}5$m/s and at the optimal operating point, $(\lambda_{opt}, C_{pmax})$that is to say at the maximum power supplied by the column of three turbines of 2062 W corresponding to the optimal average rotation speed of 7.25 rad/s, Figure 10-c shows the evolution of the torques as a function of the azimuth position of the blades. The three offset turbines column torque rosette oscillates between 361.88 Nm and 408.79 Nm while the other with three non-shifted turbines varies greatly between 233.27 Nm and 457.02 Nm. When the three turbines are offset, we observe on the torque rosette the images of the 9 blades (Figure 10-c). The presence of two driving zones and two braking zones, according to the operating principle detailed in section 2.2.2 (Figure 4), is noted in the evolution of the torques.

The simulation of the complete chain (turbine column coupled to the electrical chain) shows us that, without regulation, the rotation speed of PMSG oscillates remarkably. With non-offset turbines, it oscillates at higher amplitude than with offset turbines according to Figure 11a. The turbines column control systems (Figure 11b and Figure 12) make it possible to attenuate this vibration of the rotation speed. MPPT Neuro-fuzzy regulation is more efficient compared to MPPT with optimal TSR. Indeed, unlike the MPPT control system with optimal TSR which uses the constant reference rotation speed according to formula (3). The MPPT Neuro-fuzzy control provides the variable reference rotation speed allowing it to obtain the rotation speed of PMSG smoother from the response time of the PI correctors according to Figure 12. Furthermore, with Neuro-fuzzy MPPT control the electromagnetic torque is well combined with the torque of the turbines column from the response time of the correctors (Figure 13-b and Figure 13-d) but they have more separation in the presence of the MPPT control with optimal TSR (Figure 13-a and Figure 13-c).

The impacts of the torques were observed on the envelopes of the currents in the real benchmarks (a, b, c) and are shown in Figure 14. The currents are, in accordance with the results encountered in the literature, the images of the couples. The envelopes of the voltage amplitudes shown in Figure 15-a and Figure 15-b in the real benchmarks (a, b, c) for the tidal turbines column equipped with a MPPT control system with optimal TSR are less smooth compared to those relating to the tidal turbines column equipped with the Neuro-fuzzy MPPT regulation. The latter must be compared with other MPPT control strategies in order to judge its performance.

Introduction related your research work Introduction related your research work Introduction related your research work Introduction related your research work Introduction related your research work Introduction related your research work Introduction related your research work.

5. CONCLUSION

We determined by the Double Multiple Stream Tube (DMST) Model, the power coefficient and the mechanical torque of the column of three turbines with vertical axis of radius of 455mm and height of 824mm. For a flow of 1 .5 m/s corresponding to the maximum average power coefficient, it provides oscillating torques between 361.88 Nm and 408.79 Nm for offset turbines and between 233.27 Nm and 457.02 Nm for non-shifted turbines.

With these torques, the simulation of the entire column of three turbines and electric chain made it possible to observe that with MPPT neuro-fuzzy control system, the PMSG provides smoother electromagnetic quantities compared to the tidal turbine equipped with optimal TSR MPPT. Then, the neuro-fuzzy MPPT control strategy performs better than that of optimal TSR MPPT.

The MPPT neuro-fuzzy control strategy of the column of the three turbines is carried out with the instantaneous reference rotation speed while with MPPT optimal TSR is carried out at constant reference rotation speed. The neuro-fuzzy MPPT method which provides the instantaneous reference rotation speed made it possible to improve these results. Its comparison with other methods is interesting.

APPENDIX

Table -1: Turbines parameter

Setting	Symbol	Quantity	Unit
Speed of ocean currents	U_∞	1.5	[m/s]
Rope length	VS	156	[mm]
Turbine radius	R	455	[mm]
Impeller height	H	824	[mm]
Pitch angle	β	0	[°]

6. REFERENCES

[1]. H. Baccar et al, “Maximization of the Efficiency of a Wind Generator Based on a Permanent Magnet Synchronous Generator”, https://www.researchgate.net/publication/320347285, 2017

[2]. T. Randriamaitso, S. N. Rhevihaja, F. P. Andriniriniaimalaza, C. Andrianantenaina and T. Totozafiny “Impact study of a Vertical Axis Tidal Turbines Column's Torques on the Electromechanical Outputs of a Permanent Magnet Synchronous Generator”, Article, American Journal of Sciences and Engineering Research, E-ISSN - 2348 – 703X, Volume 6, Issue 6, 2023, www.iarjournals.com.

[3]. M. Dansoko, "Modeling and nonlinear control of tidal turbines coupled to an electrical network", Doctoral Thesis, University Paris 13-Sorbonne Paris-Cité, 2014.

[4]. AM Andreica, "Energy optimization of tidal conversion chains – modeling, controls and experimental achievements", Doctoral Thesis, InstitutPolytechnique de Grenoble, 2009.

[5]. A. Seck, “Optimization and control of a five-phase generator for tidal turbine applications”, Doctoral thesis, University of Nantes, 2019.

[6]. T. Randriamaitso, R. Manasina, FP Andriniriniaimalaza and JM Razafimahenina “Study of the torque impact on the Permanent Magnet Synchronous Generator voltages output for a vertical axis tidal turbine”, Article, International Journal of Innovative Science, Engineering & Technology (IJISET), Flight. 8 Issue 7, July 2021, ISSN (Online) 2348 – 7968 | Impact Factor (2020) – 6.72, www.ijiset.com.

[7]. M. Andreica, S. Bacha, D. Roye and J. Guiraud, "Integration of a tidal turbine into the network, MPPT and energy quality", Article, Revue des Energies Renewables Vol. 11 No. 4 (2008) 493 – 502.

[8]. P. Delafin, "Analysis of transitional flow on a hydrofoil. Application to transverse axis tidal turbines with active control of the pitch angle", Doctoral thesis, University of Western Brittany, 2014.

[9]. T. Jaquier, "Transverse flow hydropower plants: Development of a HARVEST prototype in canal", Doctoral thesis, University of Grenoble, 2011.

[10]. L. Guangnian, C. Qingren and G. Hanbin, "An Unsteady Boundary Element Model for Hydrodynamic Performance of a Multi-Blade Vertical-Axis Tidal Turbine", Article, www.mdpi.com/journal/water, Water 2018, 10, 1413.

[11]. M. Wen, Y. Ren and N. Srikanth, "Review of Maximum Power Point Tracking Algorithm for Tidal Turbine Generator", Proceedings of 3rd Asian Wave and Tidal Energy Conference 2016 (AWTEC 2016)

[12]. Billel MEGHNI “Contribution to improving the performance of a wind energy chain”. Doctoral thesis, Badji Mokhtar Annaba University, 2015 .

[13]. A. MIRECKI. “Comparative study of energy conversion chains dedicated to a small power wind turbine”. Doctoral thesis, Institut National Polytechnique de Toulouse, 2005.

[14]. W. Jaikhang, S. Tunyasrirut, "Artificial Intelligent Tuning PI Controller on Wind Turbine System with Three-Phase Grid Connected System", Article, Indonesian Journal of Electrical Engineering and Informatics (IJEEI). Flight. 7, No. 4, pp. 703~720, ISSN: 2089-3272, DOI: 10.11591/ijeei.v7i4.1329, 2019.
[15]. M. Aimene, "System services and management of transient energy interactions in an offshore wind farm", Doctoral thesis, Normandie University, 2016.
[16]. S. Apelfröjd, R. Ekström, K. Thomas and M. Leijon, "A Back-to-Back 2L-3L Grid Integration of a Marine Current Energy Converter", Article, Energies 2015, 8, 808-820; doi:10.3390/en 8020808, ISSN 1996-1073, www.mdpi.com/journal/energies.
[17]. S. Toumi, Y. Amirat, E. Elbouchikhi, M. Trabelsi, M. Benbouzid, M. FaouziMimouni, "A comparison of fault-tolerant control strategies for a PMSG-based marine current turbine system under generatorside converter faulty conditions", Article , Journal of Electrical Systems (JES), 13-3 (2017): 472-488.
[18]. D. Ikni, MS Camara, MB Camara, B. Dakyo, H. Gualous. "Permanent Magnet Synchronous Generators for Large Offshore Wind Farm Connected to Grid - Comparative Study between DC and AC Configurations", Article, INTERNATIONAL JOURNAL OF RENEWABLE ENERGY RESEARCH, DjamelIkni et al., Vol.4, No.2, 2014.
[19]. N. Batista1, R. Melicio and V. Mendes, "Darrieus-type vertical axis rotary-wings with a new design approach grounded in double-multiple stream tube performance prediction model", Article, AIMS Energy, 6(5): 673–694, http://www.aimspress.com/journal/energy, 2018.
[20]. HE Saber, EM Attia and HA El Gamal, "Analysis of Straight Bladed Vertical Axis Wind Turbine", Article, International Journal of Engineering Research & Technology (IJERT), ISSN: 2278-0181, Vol. 4 Issue 07, July-2015.
[21]. R. Manasina, "Numerical modeling and optimization of vertical axis tidal turbines with evolutionary methods", Doctoral thesis, Doctoral School of Physics and Applications, University of Antananarivo Madagascar, 2016.
[22]. AM Biadgo, A. Simonovic, D. Komarov and S. Stupar, "Numerical and Analytical Investigation of Vertical Axis Wind Turbine", Article, Faculty of Mechanical Engineering, Belgrade, FME Transactions (2013) 41, 49-58.
[23]. HQ Minh, N. Frédéric, N. Essounbouli, A. Hamzaoui, "Control of permanent magnet synchronous generator wind turbine for standalone system using fuzzy logic", Article, https://www.researchgate.net/publication/264922117, EUSFLAT- LFA 2011.
[24]. Z. Zhou, F. Sculler, JF Charpentier, M. Benbouzid, T. Tang, "Power Smoothing Control in a Grid-Connected Marine Current Turbine System for Compensating Swell Effect", Article, IEEE TRANSACTIONS ON SUSTAINABLE ENERGY, 2013, 4 (3), pp.816-826.
[25]. S. Mitchell1, I. Ogbonna1, and K. Volkov, "Improvement of Self-Starting Capabilities of Vertical Axis Wind Turbines with New Design of Turbine Blades," Article, Sustainability 2021, 13, 3854, https://www.mdpi.com/journal/sustainability.
[26]. G. Abdalrahman, W. Meleka, F. Lienb, "Pitch angle control for a small-scale Darrieus vertical axis wind turbine with straight blades (H-Type VAWT)", Article, Renewable Energy 114 (2017) 1353 – 1362.
[27]. J. Bossard, "Experimental characterization of dynamic stalling in transverse flow tidal turbines using the PIV (Particle Image Velocimetry) method. Comparison with results from numerical simulations", Doctoral thesis, University of Grenoble, 2012.